Remarks

Claims 1-51 were originally filed in this application.

Without prejudice or disclaimer, claims 39-51 were previously withdrawn from consideration as being directed to a non-elected invention.

To facilitate prosecution of this application claims 39-48 and 50-51 are currently canceled without prejudice or disclaimer.

New claims 52-61 are added without introducing new matter. Support for these new claims can be found throughout the specification, claims and drawings, as originally filed including, for example, at pages 8-14 and FIGS. 2A-2D.

Claims 1, 2, 10, 16, 17, 18, and 34 are currently amended without introducing new matter. Support for the amendments can be found throughout the originally filed specification, claims, and drawings.

As a result, claims 1-38 and 52-61 are pending for examination with claims 1, 10, 20, 34, 52, and 58 being independent claims.

Rejections Under 35 U.S.C. § 103

Claims 1-38 are rejected under 35 U.S.C. § 103(a) as obvious over the disclosure of Rela in U.S. Patent No. 6,607,668 B2 (hereinafter "Rela") and further in view of the disclosure of Sato in EP 1 172 145 A2 (hereinafter "Sato").

Applicants disagree that claims 1-38 would have been obvious over Rela in view of Sato because no proper *prima facie* case of obviousness has been presented.

Rela discloses a water purifier using membranes, ion exchange resins and electricity to remove ionic, organic and suspended impurities from water to produce high quality, pure

water. (Rela at Abstract.) Raw water is pretreated prior to primary and secondary processing. For example, in FIG. 1, which is reproduced below, Rela teaches a water purification process with a first pretreatment module with a sediment pre-filter module 10 with pressure sensors 14 and 16. (Rela at column 5, lines 46-54 and column 6, lines 15-17.)

After particles are removed in pre-filter module 10, water is directed through a conduit 18 to a softener module 20 which removes hard minerals. (Rela at column 6, lines 38-44.) From softener module 20, water is directed to a de-chlorination module 28 which includes an ultraviolet sterilization and total organic carbon reduction stage 28a and a sediment removal and de-chlorination stage 28b. (Rela at column 7, lines 41-49.) Pretreated and preconditioned water from the module 28 is introduced into a primary purification stage. Water from module 28 flows to a pressurization pump module 36 with a pump 38. (Rela at column 8, lines 36-41.) Pump 38 provides pressurized water to a reverse osmosis module 46 which separates the water into purified water, permeate, and concentrated wastewater, concentrate. (Rela at column 9, lines 4-17.) The concentrate is divided into a recycle stream, which is directed into primary processing module with feed water, and a waste stream, which is directed to a local waste system. (Rela at column 9, lines 23-41.) The permeate is directed to a secondary processing module with an electrodeionization module 54. (Rela at column 9, lines 18-22 and column 10, lines 3-11.) Product, pure water, from electrodeionization module 54 is passed through a final post-treatment conditioning module 56 which sterilizes the pure water. (Rela at column 10, lines 47-61.)

A control system (not shown) calculates the required electrical voltage and current required by the electrodeionization module 54 and automatically adjusts each to achieve optimum water quality. (Rela at column 10, lines 24-46.)

FIG. 1

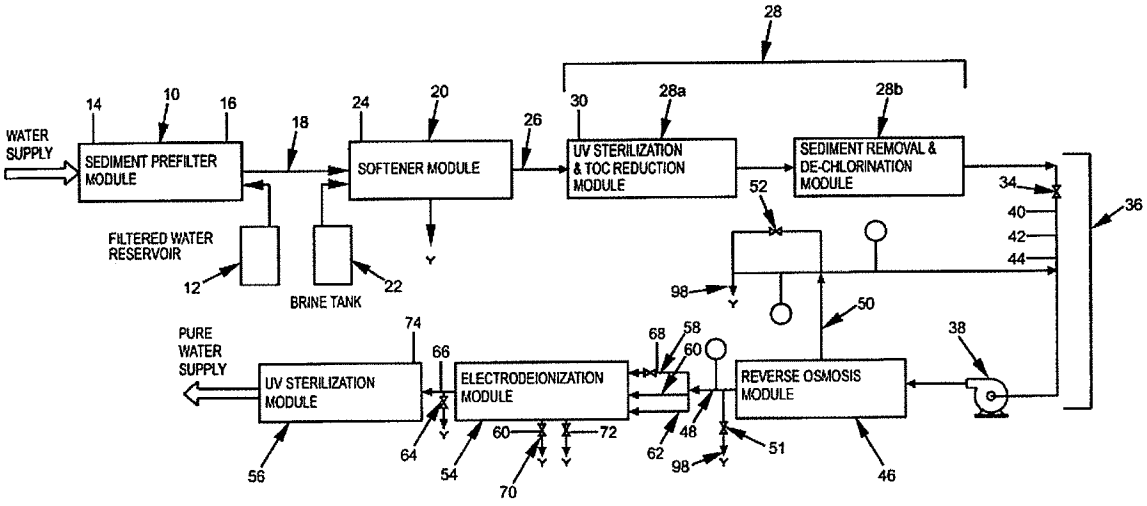

Sato discloses an electrodeionization apparatus wherein feed water is fed through an inlet 6 into a desalting compartment 8, flows around an end 4a of an anion exchange membrane 4, which surrounds an anode 2a; the feed water then enters into a portion defined between the anion exchange membrane 4 and a cation exchange membrane 5, and further flows around an end 5a of the cation exchange membrane 5, which surrounds a cathode 3a. (Sato at paragraphs [0028] *et seq.* with reference to FIG. 1, which is reproduced below.) The water then further flows around ends 4b, 5b of ion exchange membranes 4 and 5 surrounding another anode 2b and another cathode 3b, and then flows out through a product water outlet 7. (Sato at paragraphs [0038]-[0039].) A part of the product water is supplied to the concentrated water circulating within the concentrating compartments 30 and 40. (Sato at paragraphs [0038]-[0040].) A part of the concentrated water flowing out of the concentrating compartments 30 and 40 is added to concentrated water circulating within the concentrating compartments 10 and 20. (Sato at Abstract and at paragraphs [0028] *et seq.*) Silica concentration is thus reduced in the concentrated water in the concentrating compartment nearest the outlet. (Sato at paragraphs [0011] and [0042].)

Fig. 1

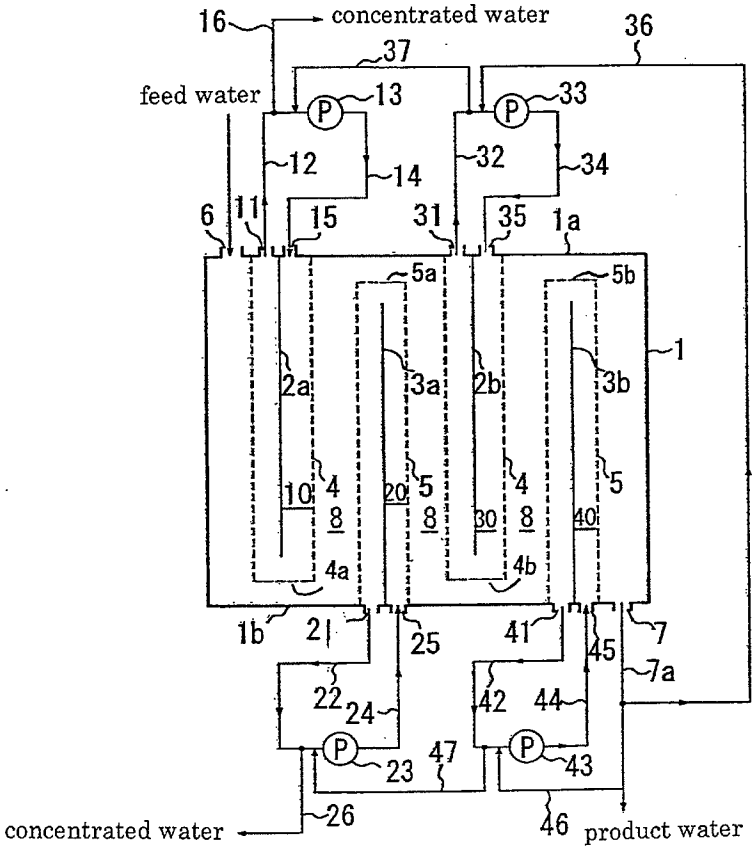

No valid *prima facie* case of obviousness has been presented because one skilled in the art would not have been motivated to modify the system of Rela with the system of Sato and, even if the references could have been combined, the resultant combination would fail to disclose each and every limitation in the manner recited in each of claims 1-38.

As noted, Sato discloses an electrodeionization apparatus configured to address silica removal whereas Rela discloses that purified water from a reverse osmosis module is further purified to produce high quality, pure water and thus requires that the reverse osmosis module be disposed upstream of the electrodeionization module. Rela further notes that upstream unit operations are utilized to soften water introduced into the reverse osmosis module and the electrodeionization device. For example, a sediment pre-filter module 10 and softener module 20 are utilized to remove hardness species from the supply water. (Rela

at column 6, lines 29-58.) Thus, Rela's system removes hardness species that would otherwise precipitate or form scale on membranes of the reverse osmosis module. Notably, one skilled in the art would understand that Rela's approach is consistent with silica scaling issues associated with reverse osmosis unit operations and accordingly provides upstream unit operations that remove scaling species upstream of the reverse osmosis.[1] One skilled in the art would also have recognized that because Rela's electrodeionization apparatus is disposed downstream of the reverse osmosis apparatus, it would not have silica removal concerns, and any advantages associated with incorporating any silica removal systems would be irrelevant. Thus, one skilled in the art would have recognized that devices and techniques directed to silica removal would not be a relevant objective of or provide any advantages in Rela's electrodeionization device. Because there is no identified need to solve a silica problem in the electrodeionization device of Rela, one skilled in the art would not have incorporated Sato's disclosure directed to silica removal. (See KSR Int'l Co. v. Teleflex Inc., 127 S.Ct. 1727 (2007) (an invention may have been obvious if there was a need to solve a problem and a finite number of identified, predictable solution).)

Therefore, the alleged *prima facie* case of obviousness is improper because the averred motivation to incorporate Sato's silica removal techniques is irrelevant in the electrodeionization device in the system disclosed by Rela.

Even if the references could have been combined, the *prima facie* case of obviousness is still improper for failing to recite each and every limitation in the manner claimed.

Each of Rela and Sato does not disclose a treatment system comprising an electrochemical device comprising a first compartment with a first compartment inlet and a first compartment outlet, and a second compartment with a second compartment inlet and a second compartment outlet; a first liquid circuit fluidly connecting the first compartment inlet

[1] See for example, an article by H. Corbin entitled Silica, Hardness, SDI and Colloids Process Removal Technology," a copy of which is attached as Appendix A, and an article by X. Zhu *et al.* entitled "Colloidal Fouling of Reverse Osmosis Membranes: Measurements and Fouling Mechanisms," a copy of which is attached as Appendix B.

to the first compartment outlet through a liquid reservoir and a first pump. Although Rela discloses a reservoir, Rela explains that the pure water reservoir 12 provides a high velocity water stream in a direction opposite the flow of supply water through the tubular element housing of sediment pre-filter module 10. (Rela at column 5, line 66-column 6, line 8.) Thus, reservoir 12 serves to store water but is not fluidly connected to an electrochemical device nor provides water to an electrochemical device.

Indeed, one skilled in the art would not have been motivated to effectively mix treated water with water to be treated in a reservoir. Significantly, none of the references recognizes that by circulating treated water through a reservoir, lower capital costs can be realized because a relatively smaller device can be used while still providing water having desirable characteristics. (See for example, Specification at page 16, lines 13 *et seq.*, and at the Example.)

Thus, any combination of Rela and Sato would fail to disclose each and every limitation in the manner recited in independent claim 1.

Therefore, the subject matter of independent claim 1 would not have been obvious because the alleged *prima facie* case of obviousness is improper for failing to disclose each and every limitation recited therein.

The respective subject matter of each of dependent claims 2-9, each of which directly or indirectly depends from independent claim 1 would also not have been obvious for at least the same reasons.

Each of Rela and Sato also does not disclose a treatment system comprising an electrochemical device fluidly connected to a point of entry, and comprising a first compartment comprising a first compartment outlet and a first compartment inlet, and a second compartment comprising a second compartment outlet and a second compartment inlet; and a water reservoir fluidly connected to the point of entry and to at least one of the first compartment inlet and the second compartment inlet. Thus, any combination of Rela

and Sato would fail to disclose each and every limitation in the manner recited in independent claim 10.

Therefore, the subject matter of independent claim 10 would not have been obvious because the alleged *prima facie* case of obviousness is improper for failing to disclose each and every limitation recited therein.

The respective subject matter of each of dependent claims 11-19, each of which directly or indirectly depends from independent claim 10, would also not have been obvious for at least the same reasons noted above.

Each of the cited references fails to disclose a method of treating a liquid comprising establishing a first liquid circuit having liquid to be treated flowing therein from a reservoir to a first compartment inlet of an electrochemical device through a first pump. Thus, any combination of Rela and Sato would fail to disclose each and every limitation in the manner recited in independent claim 20.

Therefore, the subject matter of independent claim 20 would not have been obvious because the alleged *prima facie* case of obviousness is improper for failing to disclose each and every limitation recited therein.

The respective subject matter of each of dependent claims 21-33, each of which directly or indirectly depends from independent claim 20, would also not have been obvious for at least the same reasons noted above.

Each of the references also fails to disclose a method of treating water comprising introducing at least a portion of water to be treated into a reservoir, passing at least a portion of water to be treated through a first compartment of an electrodeionization device, introducing at least a portion of the treated water into the reservoir, and reversing the polarity of an applied electric field through the electrodeionization device. Thus, any combination of

Rela and Sato would fail to disclose each and every limitation in the manner recited in independent claim 34.

Further, one skilled in the art would recognize that the Sato's device cannot be operated with reversing electric fields because electrode 2a is isolated by anion exchange membrane 4 and rendering electrode 2a as a cathode (which Sato discloses as an anode) would not allow cationic species to be collected in compartment 6 by the anion membrane 4.

Therefore, the subject matter of independent claim 34 would not have been obvious because the alleged *prima facie* case of obviousness is improper for failing to disclose each and every limitation recited therein.

The respective subject matter of each of dependent claims 35-38, each of which depends from independent claim 34, would also not have been obvious for at least the same reasons noted above.

Accordingly, reconsideration and withdrawal of the rejections of claims 1-38 under 35 U.S.C. § 103 is respectfully requested.

New Claims 52-61

The respective subject matter of each of new independent claim 52-61 would not have been obvious over Rela in view of Sato for at least the same reasons note above.

For example, each of Rela and Sato fails to disclose a water treatment system comprising a pressurizable reservoir having an inlet fluidly connectable to a point of entry, and an outlet fluidly connectable to a point of use; or a household water treatment system comprising a household water distribution system connected to at least one point of use, and a pressurized water reservoir fluidly connected to a point of entry and to the household water distribution system.

Conclusion

In view of the foregoing amendments and remarks, reconsideration is respectfully requested. This application should now be in condition for allowance; a notice to this effect is respectfully requested. If the Examiner believes, after this amendment, that the application is not in condition for allowance, the Examiner is requested to call the Applicants' attorney at the telephone number listed below.

If this Response is not considered timely filed and if a request for an extension of time is otherwise absent, Applicants hereby request any necessary extension of time. If there is a fee occasioned by this Response, including an extension fee that is not covered by an enclosed check, please charge any deficiency to Deposit Account No. 50/2762.

Respectfully submitted,
Anil D. Jha *et al.*, Applicants
By: /elias domingo/
Peter C. Lando, Reg. No.: 34,654
Elias Domingo, Reg. No.: 52,827
LOWRIE, LANDO & ANASTASI, LLP
One Main Street
Cambridge, Massachusetts 02142
United States of America
Telephone: 617-395-7000
Facsimile: 617-395-7070
Attorney for Applicants

Date: September 12, 2008

Appendix A

A copy of "Silica, Hardness, SDI and Colloids Process Removal Technology" by Horace R. Corbin, published at http://www.uswca.com/silica.pdf on December 23, 2002, is attached as Appendix A.

Appendix B

A copy of "Colloidal Fouling of Reverse Osmosis Membranes: Measurements and Fouling Mechanisms" by Xiaochua Zhu et al., published on 1997 at *Environmental Science & Technology*, vol., 31, no. 12, pp. 3554-366, is attached as Appendix B.

APPENDIX A

CORBIN
Consulting

December 23, 2002

Silica, Hardness, SDI and Colloids Process Removal Technology

By: Horace R. Corbin, P.E. - January 7, 1994
email to: horace@uswca.com
www.uswca.com

Before a raw water supply can be stripped of dissolved salts such as by reverse osmosis, pretreatment work is essential to avoid process and equipment failure. The pretreatment process must be reliable and flexible. It often must perform in a remote environment under varying and unknown conditions. It must not impose operating complexities on the site personnel.

The main pretreatment process needs are:

1. Silica, Metals and Hardness Reduction.
2. Suspended Solids and Colloid Control, Fouling Factors Minimization.
3. Scaling Reduction, Organic Removal and Biological Stabilization.

The Pretreatment Process must be flexible to respond to variations in the water supply characteristics, climatic conditions, temperature and flow. The system design often must proceed based on limited information at hand at the project start. Startup adjustment and operation must be responsive to actual site conditions encountered.

Communication, Training, Maintenance, Service and Technical Support must be accessible for the site. For practical reasons, complex issues must be kept to a minimum. However, when needed, service must be available, effective and responsive.

Thorough Operating and Maintenance Documents must be prepared in the native language of the operating staff. Often, dual language and dual dimensioned documents are required, such as Spanish/English and with Metric/Imperial dimension standards.

TECHNOLOGY FOR SIO2 REMOVAL

Silica exists in all waters in multiple chemical and physical/chemical forms. Generally, quasi-soluble silica is analyzed and reported as HSiO2- weak anion. Other forms of silica go undetected. HSiO2- is found in most natural waters at levels generally from 5-30 mg/l.

HSiO2- becomes troublesome for piping and other equipment at levels of 150 mg/l and above due to formation of hard, glass-like plating that resists removal. These factors are well understood in evaporative cooling tower applications in power generation and in similar other fields.

HSiO2- is a serious problem for reverse osmosis operation as concentration occurs at the liquid/membrane interface. Left uncontrolled, the membranes become destroyed in a short time. The problem is avoided by removing the silica prior to the Reverse Osmosis unit.

At a mine location in South America, the silica concentration in the water supply is unusually high (essentially at saturation). A large portion of the silica is removed as the first task (to ~30 mg/l). Although this silica issue is unusually difficult for most designers, it is not an unusual problem in for special plants designed to deal with it, such as for power plant operation in cooling towers.

Horace Corbin has developed the process for enabling cooling towers to reach high cycles of concentration, while stripping excess silica, calcium, magnesium, and alkalinity to maintain safe conditions. This process is also applied to unusual water supply conditions at other locations.

CAUSTIC ZONE STRIPPING

The "Caustic Zone Stripping" process employs specially arranged hardware, computer controls, programming and chemical reaction techniques for removing excess silica from water streams. The hardware includes a solids contact slurry recirculation reactor, dual media "coated adsorption" filters, precision chemical feed units, programmed computer control and complete instrumentation monitoring for assured operations.

The reactor is automatically maintained at the appropriate pH such as by caustic addition with feedback control. Silica is adsorbed from the water as calcium and magnesium are caused to precipitate. Calcium precipitates stoichiometrically as a function of the natural alkalinity in the water supply. Additional calcium can be removed if the alkalinity is insufficient, by adding soda ash. At ambient temperatures, hardness can be reduced to approximately 35 ppm.

Silica is removed in an empirical relationship as a function of Mg(OH)2 formation resulting from caustic reaction with background magnesium. Additional Silica can be removed, by adding magnesium salts, if the background magnesium is insufficient. The magnesium compounds applicable to the process include MgSO4, MgCl2, and MgO. Generally, MgSO4 is the preferred choice due to ease of use. Chemical availability often is a determining factor.

The mechanisms of silica removal in the reactor include magnesium silicate formation, adsorption of silica of the surface of Mg(OH)2 floc, and physical encapsulation of silica within the floc particles. At ambient temperatures, silica can be removed to as low as 15 mg/l. Generally, the design target is established at 30 mg/l.

Lime is used in some applications for economic considerations. This can replace some of the caustic and soda ash requirements. In many cases, caustic and soda ash cannot be completely eliminated. It's a matter of chemistry and must be review on a case by case basis. Lime use complicates operation, adds to equipment & maintenance requirements, and increases the knowledge and attention required by operators. It is often more desirable to keep the system design and equipment as simple and maintenance free as possible; even at the expense of apparent higher chemical costs.

P.O. Box 250 • Westfield, NJ 07091 • 908.232.3473 direct
908.232.4407 gen'l • 908.232.0473 fax • horace@goleader.com

In this way, the actual chemical costs can be lower as the operating efficiency proves to be higher.

Caustic is applied to the reactor at the upper reaction surface creating a stratified high pH zone. This drives Mg precipitation to extreme de-saturation level and increases process efficiency.

Soda ash is applied to the reactor in the lower reaction zone for preferential reaction with calcium to form calcium carbonate precipitate. Soda ash feed and other reactor features are arranged to minimize parasitic magnesium carbonate precipitation, which decreases efficiency. Excess precipitates are blown down from the reactor by gravity; paced by the control system as a function of treated volume.

Considerable design attention is required ensure sludge management and removal as the volumes can become substantial and overload undersized equipment.

Similarly, chemical feeds must be precisely paced by the controlled system. The caustic is a function of pH set-point while the soda ash and Mg salts are paced with flow. Dosing level is preset by the operator as a function of the desired degree of treatment.

In many cases, the reactor effluent displays a characteristic white haze due to the presence of microscopic Mg(OH)2 particle de-saturation. This carries forward to the filtration system by conveyance of a clearwell tank and transfer pumping system.

By design, the Mg(OH)2 particles become enmeshed in the filter media and act as polishing adsorption media. This achieves a high degree of silica extraction and SDI (silt density index) reduction. The filter effluent is sparkling clear, with a very low SDI, and at the target silica content.

The filter system is washed automatically, once per day. The Mg(OH)2 particles are light, non-scaling, and easily removed by the backwashing action provided. Washing is invoked by the control system programming once per day per filter for approximately 15 minutes. During this period, the service flow is temporarily suspended. The control system staggers the washing action of individual filter units throughout the day such that system interface tanks can continuously provide product water for the users.

The technical details described above are transparent to the operating personnel. Essentially, most actions occur automatically without adjustment required or desired. The operator's main duties include system surveillance, preventative maintenance, and repair.

It is desirable to equip the site with basic water chemistry laboratory analytical apparatus and to provide training to operating personnel on its' use. A water analysis kit (such as by Hach), jar test kit, and SDI test equipment are recommended along with

related glassware and reagents. It is highly desirable to have email, Internet and telefax service in the operating control room to facilitate technical service.

The equipment required for plant designs as discussed within this document is of common use throughout the world. Spare parts are readily available. No unusual maintenance requirements are involved. The most important ingredient is proper system design, quality construction, process knowledge, experience and training.

Contact the writer for specific design details and assistance with your project.
horace@uswca.com

by
Horace R. Corbin, P.E.
January 7, 1994
Updated December 23, 2002

P.O. Box 250 • Westfield, NJ 07091 • 908.232.3473 direct
908.232.4407 gen'l • 908.232.0473 fax • horace@goleader.com

APPENDIX B

Environ. Sci. Technol. 1997, 31, 3654–3662

Colloidal Fouling of Reverse Osmosis Membranes: Measurements and Fouling Mechanisms

XIAOHUA ZHU AND
MENACHEM ELIMELECH*
Department of Civil and Environmental Engineering, University of California, Los Angeles, California 90095-1593

The effect of chemical and physical interactions on the fouling rate of cellulose acetate and aromatic polyamide composite reverse osmosis (RO) membranes by silica colloids is investigated. Results of fouling experiments using a laboratory-scale unit demonstrate that colloidal fouling rate increases with increasing solution ionic strength, feed colloid concentration, and permeate water flux through the membrane. It is demonstrated that the rate of colloidal fouling is controlled by a unique interplay between permeation drag and electric double layer repulsion; that is, colloidal fouling of RO membranes involves interrelationship (coupling) between physical and chemical interactions. For solution chemistries typical of natural source waters, permeation drag under normal operating conditions plays a more significant role than chemical interactions and may ultimately control the rate and extent of colloidal fouling. In addition to permeation drag, it is shown that membrane surface morphology has a marked effect on colloidal fouling. The higher fouling propensity of composite polyamide RO membranes compared to cellulose acetate RO membranes is attributed to the pronounced surface roughness of the composite membranes. Implications of the results for developing means to reduce colloidal fouling of RO membranes are discussed.

Introduction

Advances in membrane technology along with the emergence of new and more stringent water quality regulations have stimulated a resurgence in the use of reverse osmosis (RO) for water supply augmentation. RO membranes are presently being used in such diverse applications as sea water and brackish water desalination, removal of inorganic and organic dissolved species from drinking water supplies, and reclamation of municipal and agricultural wastewaters (*1*). A major obstacle for the widespread use of RO technology is the problem of colloidal fouling (*1, 2*). Therefore, a fundamental understanding of the chemical and physical mechanisms governing the fouling of RO membranes by aquatic colloids is of paramount practical importance.

Colloidal particles are ubiquitous in natural waters. Colloids cover a wide size range, from a few nanometers to a few micrometers. Examples of aquatic colloids are clay minerals, colloidal silica, iron, aluminum, and manganese oxides, organic colloids and suspended matter, and calcium carbonate precipitates. In the pH range of natural waters, most colloids carry a negative surface charge. The surface charge of aquatic colloids reflects their surface chemical properties and the chemical composition of natural waters (*3*).

During membrane fouling, colloids accumulate on the membrane surface or within the membrane pores and adversely affect both the quantity (permeate flux) and quality (solute concentration) of the product water. When analyzing colloidal fouling of pressure-driven membranes, it is important to distinguish between two cases. For RO, nanofiltration (NF), and perhaps "tight" ultrafiltration (UF) membranes, colloidal fouling is caused by the accumulation of particles on the membrane surface in a so-called cake layer. This cake layer provides an additional hydraulic resistance to water flow through the membrane and, thus, reduces the product water flux (*4*). For microfiltration (MF) membranes, pore plugging by colloidal particles can be an important fouling mechanism, in addition to particle accumulation on the membrane surface (*5*). The extent of pore plugging and cake layer formation depends on the relative size of the particles compared to the membrane pore size. Because RO membranes are considered "non-porous", the sole mechanism of RO colloidal fouling is by cake layer formation.

Systematic studies on the role of physical and chemical interactions in colloidal fouling of RO membranes are rather scarce. Winfield (*6, 7*) studied the fouling of cellulose acetate RO membranes by a secondary wastewater effluent. It was suggested that dissolved organic substances play a much more significant role in membrane fouling than large suspended particles. However, this study did not distinguish between the contributions of dissolved organic species and small submicrometer-sized colloidal particles to membrane fouling. Furthermore, the role of chemical and physical interactions and the mechanisms involved in membrane fouling were not delineated. In a later study by Cohen and Probstein (*8*), the fouling rate of cellulose acetate RO membranes by freshly formed colloidal ferric hydroxide was reported. Fouling was correlated to the foulant layer growth, and a linear dependence between permeate flux and foulant layer thickness was found for the initial stages of fouling. The solution chemistry in their study, however, was limited to deionized water so that the role of chemical and physical interactions in membrane fouling could not be systematically investigated. More recently, Zhu and Elimelech (*4*) investigated the effect of solution chemistry on the fouling rate of cellulose acetate and composite polyamide RO membranes by aluminum oxide colloids. They demonstrated that colloidal fouling is controlled by colloid–membrane interaction, and by the interaction of suspended colloids with previously retained colloids. Their study, however, cannot be generalized to other colloidal particles because the aluminum oxide colloids under the solution pH investigated were positively charged, whereas most aquatic colloids are negatively charged. Furthermore, the interrelation between physical and chemical interactions was not systematically investigated in that study.

The objective of this paper is to systematically investigate the effects of chemical and physical interactions, and the interrelation between such interactions, on the rate of fouling of cellulose acetate and composite polyamide reverse osmosis membranes by silica colloids. On the basis of the obtained experimental fouling results, the measured chemical and physical properties of the silica colloids and RO membranes, and theoretical analyses of colloid transport and deposition onto permeable surfaces, a mechanistic explanation is proposed for the role of chemical and physical interactions in colloidal fouling of RO membranes. The causes for the higher propensity of composite polyamide RO membranes to colloidal fouling, compared to cellulose acetate RO membranes, are further elucidated.

* Author to whom correspondence should be addressed; fax: (310) 206-2222; e-mail: elim@seas.ucla.edu.

S0013-936X(97)00400-8 CCC: $14.00

Materials and Methods

Silica Colloids and RO Membranes. Commercial silica colloids (Aerosil 200, Degussa Corp., Akron, OH) were used as a model colloidal foulant. The colloidal silica was supplied in a powder form and was used as obtained with no further treatment. It has a BET surface area in the range of 175 to 225 m^2/g, a silanol group density of 2.6 per nm^2, and a density of 2.2 g/cm^3 (*9*). The mean hydrodynamic radius of the colloids, as determined by dynamic light scattering (Nicomp Model 370, Particle Sizing Systems, Santa Barbara, CA), was 120 nm.

Thin-film composite (Fluid Systems Corp., San Diego, CA) and cellulose acetate (Desalination Systems, Escondido, CA) RO membranes were used in this investigation. The low-pressure thin-film composite membrane (denoted as "TFCL" by the manufacturer) is an interfacially polymerized aromatic polyamide membrane. The membrane was supplied as a wet flat sheet and stored in a 0.75% sodium metabisulfite solution at 5 °C. The cellulose acetate membrane (denoted as "CE" by the manufacturer) is a blend of cellulose diacetate and triacetate; it was supplied as a dry flat sheet and stored at room temperature.

Reagents and Chemical Solutions. All chemicals used were reagent grade (Fisher Scientific, Pittsburgh, PA) and were used without purification. Solutions and silica suspensions were prepared with deionized water (Nano Pure II, Barnstead, Dubuque, IA) having a conductivity of less than 1 μS/cm when in equilibrium with atmospheric CO_2. Colloid stock suspensions (1000 mg/L) were prepared by dispersing silica powder in deionized water via intense mixing and ultrasonication for 30 min.

Characterization of Colloids and Membranes. The electrophoretic mobility of the silica colloids under various chemical conditions was measured by microelectrophoresis (Lazer Zee Model 501, Pen Kem Inc., Bedford Hills, NY). Zeta potentials of the RO membranes were determined by a streaming potential analyzer (BI-EKA, Brookhaven Instruments Corp., Holtsville, NY). Details on the instrument and the procedures for streaming potential measurements are given elsewhere (*10, 11*).

The stability ratio of the silica colloids was determined by light extinction measurements (*12*). A UV–vis spectrophotometer (HP 8452A, Hewlett Packard, Palo Alto, CA) connected to a rapid kinetics, stopped-flow accessory (SFA-20, Hi-Tech Scientific, Salisbury, U.K.) was used to measure the change in the light extinction of the colloids as a function of time at various solution chemistries; a wavelength of 546 nm was used in all experiments. The deionized water used in the experiments was boiled prior to use to remove small air bubbles that might influence the measurements of coagulation kinetics. Before each coagulation experiment, the colloidal suspension was subjected to ultrasonication for a few minutes. The temperature in the coagulation experiments was maintained at 20 ± 0.1 °C with the use of a recirculation bath (Isotemp refrigerated circulator, Model 910, Fisher Scientific, Pittsburgh, PA).

The surface roughness of the membranes was characterized by SEM and atomic force microscopy (AFM). The AFM images were obtained with a NanoScope III scanning probe microscope (Digital Instruments, Santa Barbara, CA) in the tapping mode.

Fouling Experiments. A closed-loop, bench-scale RO unit was used for the fouling tests. In this system, the colloid suspension is fed to the RO membranes by a positive displacement pump (Milton-Roy Model R221, Ivyland, PA). The suspension splits into two parallel streams, feeding into duplicate membrane test cells. The rectangular cells contain membranes with dimensions of 2.5 by 6.4 cm. Temperature is controlled by circulating cooling water through a stainless-steel coil immersed in the feed tank.

Fouling experiments were carried out with colloidal silica at different solution chemistries. Before a typical RO fouling experiment, a baseline test was conducted for each membrane. A baseline test was carried out with solution chemistry and testing conditions similar to those of the fouling test but without colloidal particles. Differences between membrane performance (*i.e.*, permeate flux or salt rejection) for the baseline and the fouling tests represent the net effect of colloidal fouling.

Prior to fouling or baseline tests, the membranes were placed in the unit and were rinsed in a flow-through mode with 15 L of deionized water to remove impurities that may be attached to the membrane surface. In a typical test, the membranes were first equilibrated under normal operating pressure with deionized water for 8 h and then with a particle-free salt solution for an additional 36 h. After this equilibration period (*i.e.*, 44 h), the permeate water flux and salt rejection (measured by electric conductivity) were constant. Successful equilibration (*i.e.*, equilibration following which the water flux attained a target value within a specified accuracy) was essential for obtaining reproducible fouling experiments. Fouling experiments were initiated by adding a concentrated silica stock suspension to the feed tank to establish the desired particle concentration.

The solution pH in fouling experiments with the cellulose acetate membranes was in the range 5.4–5.6 (unbuffered). This is the optimal operation pH for cellulose acetate membranes to prevent hydrolysis of the polymer. Fouling experiments with the composite membranes were conducted at pH 7.8 via the addition of 1 mM $NaHCO_3$, which represents typical alkalinity of natural waters.

Hydrodynamic conditions in all fouling experiments remained constant. Unless stated otherwise, experiments were conducted at a transmembrane pressure of 250 psi (1724 kPa) for the thin-film composite membranes and 400 psi (2758 kPa) for the cellulose acetate membranes. These are the manufacturer's recommended pressures for typical operation of the membranes. For the tests involving foulant mass measurements and effect of surfactants, a predetermined initial flux was obtained by adjusting the transmembrane pressure at the end of the equilibration period. The temperature in all experiments was fixed at 20 °C and the cross-flow rate was set to 800 mL/min, resulting in a cross-flow velocity of 5.3 cm/s. The corresponding Reynolds number (based on cross-flow velocity and hydraulic radius of the membrane channel) was about 450.

Results and Discussion

Following a discussion on the chemical characteristics of the model membranes and colloids, the effects of several chemical and physical factors on the rate of colloidal fouling are elaborated and discussed. These results, along with theoretical analyses, are used to delineate the mechanisms of colloidal fouling.

Characteristics of Colloids and Membranes. The electrophoretic mobility of the silica colloids as a function of solution pH and ionic strength is presented in Figure 1. Consistent with previous studies (*13*), the isoelectric point of the colloidal silica is approximately at pH 3. Since solution pH in all colloidal fouling tests was either 5.4–5.6 (for the cellulose acetate membrane) or 7.8 (for the composite membrane), the surfaces of the silica colloids possessed a net negative charge during all colloidal fouling tests. As expected, the particles are less negative at higher ionic strength due to double layer compression and reduction of the Stern potential (*14*).

Colloidal stability measurements of the silica colloids were carried out to ensure that the silica colloids do not aggregate in the feed solution during the fouling experiments and to assess the colloidal interactions that develop between suspended and retained silica colloids during membrane fouling.

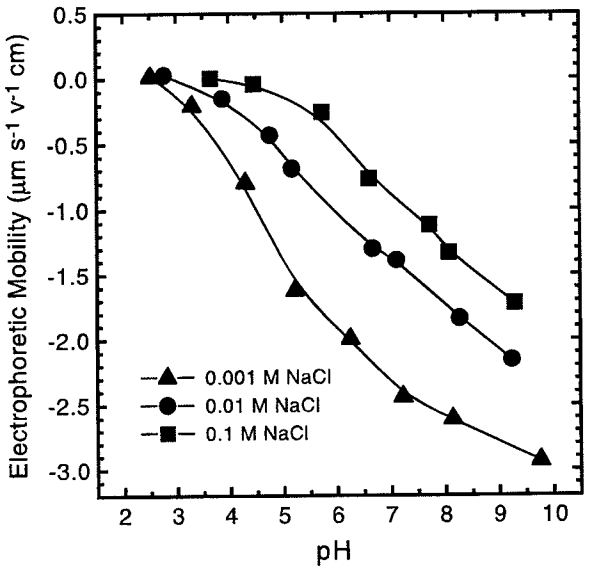

FIGURE 1. Electrophoretic mobility of silica colloids as a function of solution pH and ionic strength.

Results showed that the silica colloids are extremely stable and do not aggregate even in presence of 0.1 M NaCl in solution (*12*). The critical coagulation concentration of the colloidal suspension was about 1 M NaCl. This "anomalous" stability of the silica colloids at high salt concentration is well documented in the literature and is attributed to hydration (*15*) and steric-like (*16*) repulsive forces. A recent investigation by Israelachvili and co-workers (*16*) suggests that the unusual interfacial properties of silica surfaces are attributed to the presence of a thin (ca. 1 nm) gel-like layer of protruding silanol and silicilic acid groups that grow on the surface in the presence of water. The surface gel layer effectively shifts the outer Helmholtz plane outward and adds a monotonic short-range steric repulsion to the electrostatic double layer repulsion.

The zeta potential behavior of the thin-film composite and cellulose acetate membranes at various solution chemistries has been presented elsewhere (*11*). Both membranes exhibit characteristics of amphoteric surfaces containing acidic and basic functional groups. The isoelectric points of the composite and cellulose acetate membranes were found to be at pH 5.2 and 3.5, respectively. The difference in the zeta potential behavior is attributed to differences in the chemistry of the aromatic polyamide and cellulose acetate polymeric surfaces of the membranes. At the pH values used in all fouling experiments (5.4 or 7.8), both types of the RO membranes, as well as the silica colloids, are negatively charged. Hence, repulsive double layer interactions develop between the silica colloids, and between the silica colloids and the membrane surface.

Atomic force microscopy (AFM) images of the active layer surfaces of the composite and cellulose acetate membranes are displayed in Figure 2. The AFM images clearly show the remarkable differences between the surface morphologies of the two membranes. While the thin-film composite membrane exhibits large-scale surface roughness of ridge-and-valley structure, the cellulose acetate membrane surface is relatively smooth. The distinct roughness of the composite membranes is an inherent property of interfacially polymerized aromatic polyamide composite membranes (*17*). Upon inspecting the AFM images, one should note that the scale of the vertical *z*-axis for the two types of membranes is very different. A much larger scale *z*-axis was used for the image of the composite membrane because of the marked roughness. The roughness of the cellulose acetate membrane is on the order of a few nanometers whereas that of the composite membranes is on the order of several hundred nanometers. It will be shown later that this remarkable surface roughness of the composite membrane has a dramatic effect on the deposition rate of colloids to the membrane surface. It is worthwhile to mention that the marked difference in the surface roughness of the two membranes was also confirmed by SEM micrographs (*12, 18*).

Effect of Particle Concentration. The effect of silica colloid concentration on the fouling rate of the composite and cellulose acetate membranes at a fixed solution chemical composition is shown in Figure 3. Results are presented as relative permeate (water) flux as a function of time. The relative flux is the flux at any time during the fouling test divided by the initial water flux through the membrane, just before adding the silica colloids at the end of the 44 h equilibration period. The corresponding baseline curves are also included in this figure. The baseline data are for the relative flux in test runs with a colloid-free solution after the equilibration period. The difference between the permeate flux in the presence of colloids and the baseline represents the net contribution of colloidal particles to membrane fouling.

The results in Figure 3 show that greater flux decline is obtained at higher feed concentrations of silica colloids. As particle concentration increases, the rate of convective particle transport toward the membrane surface (*i.e.*, the product of permeate flux and particle concentration) increases and, hence, the overall rate of colloid deposition onto the membrane increases. Consequently, the amount of deposited colloids increases, resulting in higher resistance to water flow and thus reduced water flux. Comparing the relative permeate fluxes of the composite and cellulose acetate membranes reveals that, for a given particle concentration, the flux through the composite membrane decreases at a much faster rate than the cellulose acetate membrane. As will be discussed later in this paper, this behavior is attributed to the higher initial permeate flux in fouling runs with the composite membrane (see initial fluxes in figure caption) and to the difference in the surface morphologies of these two types of membranes.

To demonstrate that the permeate flux decline is directly related to the mass of colloids accumulated at the membrane surface, four separate fouling runs with the composite membrane (at 0.1 M NaCl and 90 mg/L silica colloids) were carried out for durations of 12, 24, 36, and 48 h. At the end of each of these runs, the membranes were removed from the test cells and the mass of accumulated silica colloids was determined gravimetrically. The results for the accumulated mass (per unit membrane area) as a function of time, as well as the corresponding permeate flux data, are shown in Figure 4. As total accumulated mass of particles increases, the resistance of the colloid deposit (cake) layer to water flow increases and, hence, the permeate flux decreases. For the data shown in Figure 4, after 48 h of fouling, the cake layer resistance accounts for over 50% of the total resistance (*i.e.*, membrane plus cake layer resistances) to water flow.

Effect of Permeation Rate (Drag). Figure 5 describes the relative flux as a function of time for fouling runs at different permeation rates but fixed solution chemical composition. The initial permeate flux was controlled by setting the transmembrane pressure for each fouling run to the values indicated in the figure. As shown, fouling is more severe at higher permeation rates. Since the solution chemical composition and the feed colloid concentration for the displayed fouling runs are similar, the first immediate explanation for the observed fouling behavior is the different rate of particle convective transport (product of permeation rate and colloid concentration) toward the membrane surface at the various permeation rates used. As discussed in the previous subsection, higher particle transport rate results in greater rate of

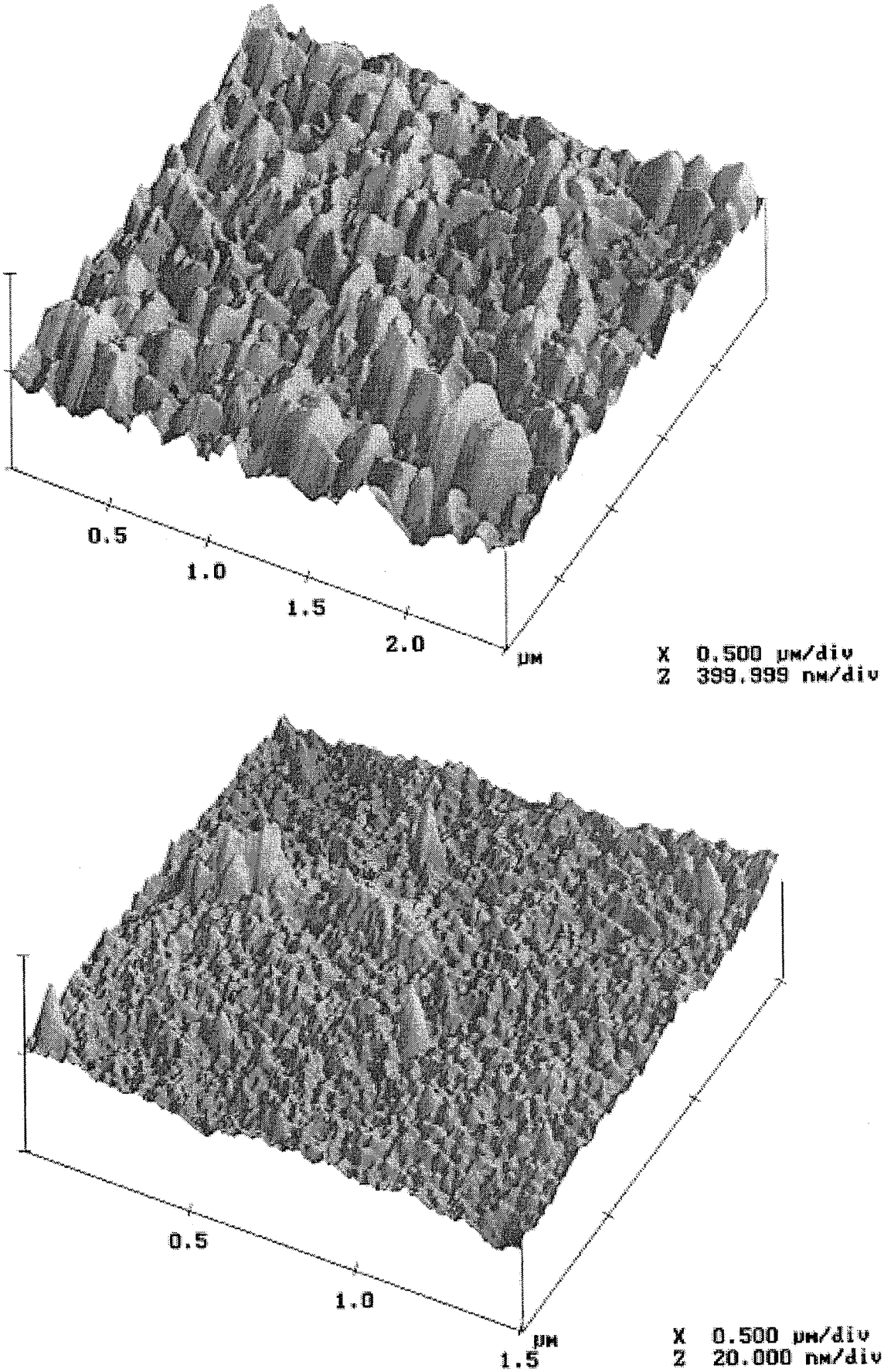

FIGURE 2. AFM images of (A) the composite RO membrane and (B) the cellulose acetate RO membrane. Note that for the composite membrane the *z*-axis scale is 400 nm per division and the *x*-axis scale is 500 nm per division; for the cellulose acetate membrane the *z*-axis scale is 20 nm per division and the *x*-axis scale is 500 nm per division.

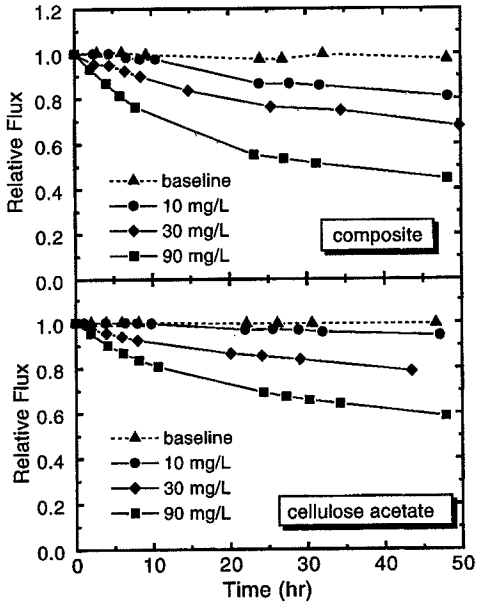

FIGURE 3. Relative flux as a function of time in fouling tests with composite and cellulose acetate RO membranes at three different particle concentrations. All experiments were conducted with 0.1 M NaCl. Experiments with the composite membrane were carried out at pH 7.8 while those with the cellulose acetate membrane were carried out at pH 5.4–5.6. The initial fluxes for runs with the composite membranes were as follows: 8.36×10^{-6} m/s (baseline), 8.60×10^{-6} m/s (10 mg/L run), 8.28×10^{-6} m/s (30 mg/L run), and 8.28×10^{-6} m/s (90 mg/L run). The initial fluxes for runs with the cellulose acetate membranes were as follows: 6.25×10^{-6} m/s (baseline), 6.50×10^{-6} m/s (10 mg/L run), 6.71×10^{-6} m/s (30 mg/L run), and 5.95×10^{-6} m/s (90 mg/L run).

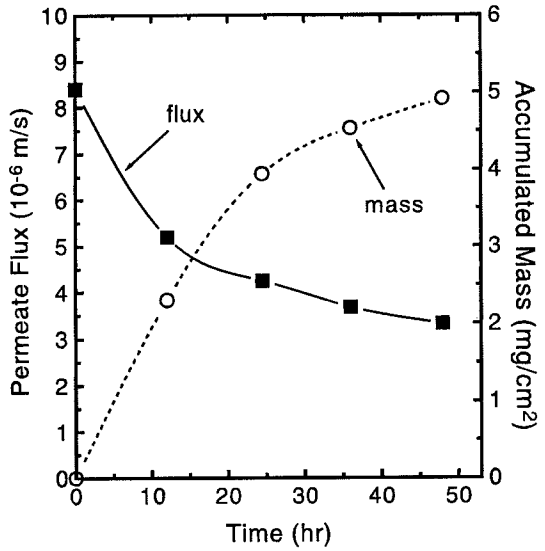

FIGURE 4. Permeate flux and accumulated mass as a function of time during fouling with the composite RO membranes. Data were collected at the end of four different fouling tests operating over periods of 12, 24, 36, and 48 h. Fouling tests were carried out with 0.1 M NaCl, silica colloid concentration of 90 mg/L, solution pH of 7.8, and applied pressure of 255 psi.

particle deposition onto the membrane surface and, subsequently, increased rate of membrane fouling.

To explore the possibility of other causes for the increased fouling rate at higher permeation rates, the fouling results are presented in terms of relative permeate flux as a function of total accumulated permeate volume rather than time (Figure 6). By this type of analysis, the differences in the particle convection rates are accounted for, and the slopes

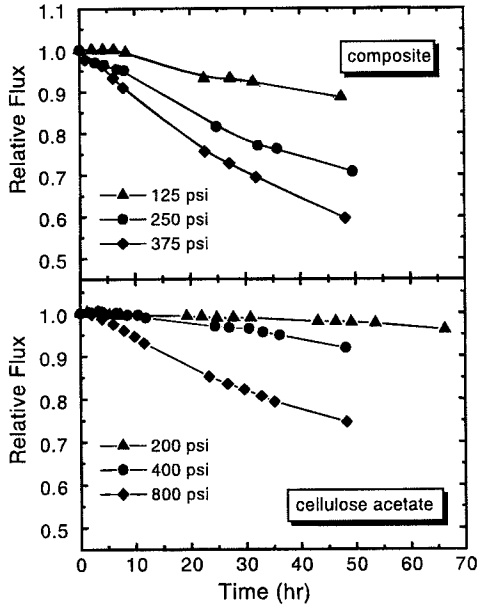

FIGURE 5. Relative flux as a function of time in fouling tests with composite and cellulose acetate RO membranes at different applied pressures (or initial permeate fluxes). All experiments were conducted with 0.01 M NaCl and 30 mg/L silica colloids. Experiments with the composite membrane were carried out at pH 7.8 while those with the cellulose acetate membrane were carried out at pH 5.4–5.6. The initial fluxes for runs with the composite membranes were as follows: 6.18×10^{-6} m/s (125 psi run), 1.07×10^{-5} m/s (250 psi run), and 1.77×10^{-5} m/s (375 psi run). The initial fluxes for runs with the cellulose acetate membranes were as follows: 3.31×10^{-6} m/s (200 psi run), 5.27×10^{-6} m/s (400 psi run), and 1.10×10^{-5} m/s (800 psi run).

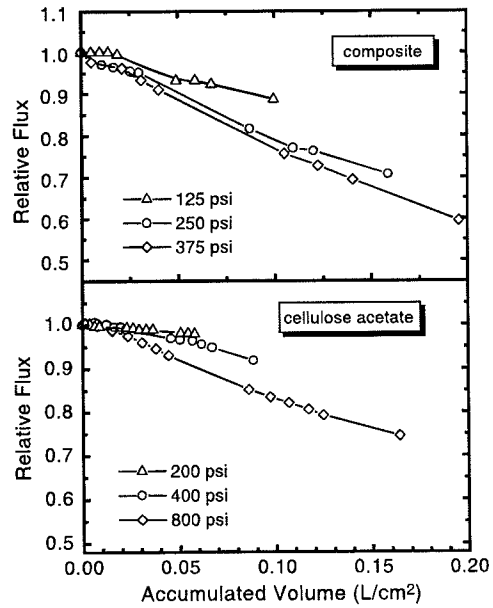

FIGURE 6. Relative flux as a function of total accumulated volume per unit membrane area for the data shown in Figure 5. Accumulated volume was obtained from integration of the permeate flux with respect to time.

of all the fouling curves should be identical if the sole effect of permeation rate is on the convective transport rate. However, as shown in Figure 6, there is still a substantial difference between the fouling curves at the various permeation rates. The difference in the fouling behavior is attributed to the so-called "permeation drag" as discussed below.

Song and Elimelech (*19*) have recently presented a theoretical investigation of particle deposition onto a perme-

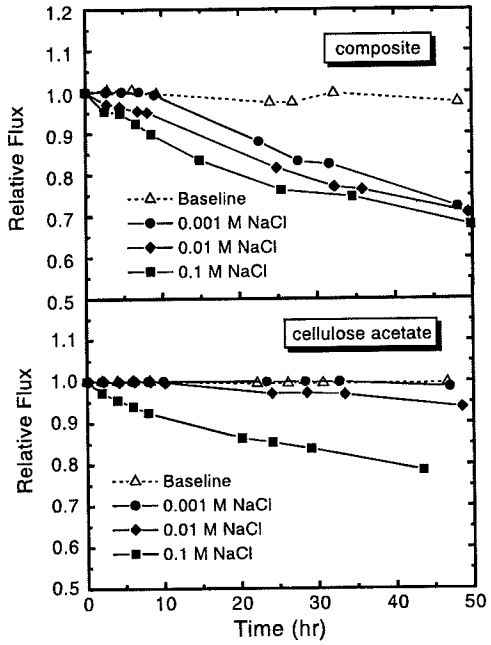

FIGURE 7. Relative flux as a function of time in fouling tests with composite and cellulose acetate RO membranes at three different solution ionic strengths. All experiments were conducted with 30 mg/L silica colloids. Experiments with the composite membrane were carried out at pH 7.8 while those with the cellulose acetate membrane were carried out at pH 5.4–5.6. The initial fluxes for runs with the composite membranes were as follows: 8.36×10^{-6} m/s (baseline), 1.02×10^{-5} m/s (0.001 M run), 1.07×10^{-5} m/s (0.01 M run), and 8.28×10^{-6} m/s (0.1 M run). The initial fluxes for runs with the cellulose acetate membranes were as follows: 6.25×10^{-6} m/s (baseline), 7.23×10^{-6} m/s (0.001 M run), 7.12×10^{-6} m/s (0.01 M run), and 6.71×10^{-6} m/s (0.1 M run).

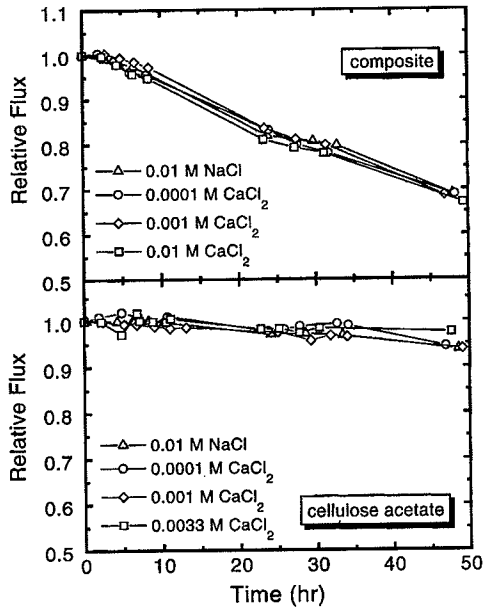

FIGURE 8. Relative flux as a function of time in fouling tests with composite and cellulose acetate RO membranes at different concentrations of divalent cations (Ca^{2+}). All experiments were conducted with 30 mg/L silica colloids and 0.01 M NaCl as a background electrolyte. Experiments with the composite membrane were carried out at pH 7.8 while those with the cellulose acetate membrane were carried out at pH 5.4–5.6. The initial fluxes for runs with the composite membranes were as follows: 1.11×10^{-5} m/s (0.01 M NaCl run), 1.10×10^{-5} m/s (0.0001 M $CaCl_2$ run), 1.13×10^{-5} m/s (0.001 M $CaCl_2$ run), and 1.15×10^{-5} m/s (0.01 M $CaCl_2$ run). The initial fluxes for runs with the cellulose acetate membranes were as follows: 7.12×10^{-6} m/s (0.01 M NaCl run), 6.48×10^{-6} m/s (0.0001 M $CaCl_2$ run), 7.04×10^{-6} m/s (0.001 M $CaCl_2$ run), and 6.14×10^{-6} m/s (0.0033 M $CaCl_2$ run).

able surface in laminar flow. Their theoretical analysis indicates that the rate of colloid deposition onto a permeable surface is controlled by an interplay between double layer repulsion and the opposing hydrodynamic force (permeation drag) resulting from the convective flow toward the membrane. The permeation drag force is proportional to the permeate flux; it acts perpendicular to the membrane surface, in an opposite direction to the double layer repulsion force. Under typical operating conditions, the permeation drag can be significant, overcoming the double layer repulsive force and resulting in particle deposition and subsequent membrane fouling. This unique mechanism, which is nonexistent in particle deposition phenomena onto impermeable surfaces, accounts for the differences in the fouling curves shown in Figures 5 and 6. Further discussion on the paramount role of permeation drag in membrane fouling will follow when the effect of ionic strength on fouling is presented.

Effect of Solution Ionic Strength. The effect of solution ionic strength on the rate of colloidal fouling is presented in Figure 7. The fouling tests were carried out at three NaCl concentrations: 0.001, 0.01, and 0.1 M. In general, fouling rate increases with increasing ionic strength. The rate and magnitude of fouling of the composite membrane by colloidal silica are more pronounced at higher ionic strengths. Fouling was significant in all runs involving the composite membrane, but only for runs at high ionic strength for the cellulose acetate membrane. No fouling was observed with the cellulose acetate membrane at an ionic strength of 0.001M.

The fouling results shown in Figure 7 can be directly interpreted by the previously discussed interplay between ionic strength (chemistry) and permeation drag (physics). At the solution pH used in the fouling experiments, both colloidal silica and membrane surfaces possess a net negative charge, and as a result, the deposition of the colloidal silica onto both the clean and fouled membrane surface is hindered by the repulsive electrostatic double layer forces. At low ionic strength, there exists a strong double layer repulsion between the newly approaching colloidal particles and the membrane surface or between approaching and previously retained particles, and the rate of fouling is controlled by the interplay between permeation drag and double layer repulsion. The permeation drag is significant for the composite membrane because of the higher initial permeation rate (see initial fluxes in figure captions); this hydrodynamic force overcomes double layer repulsion so that fouling occurs, albeit at a slower rate for the lower ionic strengths. At high ionic strengths, the double layer repulsion is significantly reduced, and the fouling rate is controlled by permeation drag. Because the initial permeation rate for the cellulose acetate membrane runs is smaller, double layer repulsion can overcome the permeation drag at low ionic strength (0.001 M) and fouling is not observed. At higher ionic strengths, the range and magnitude of the double layer repulsion is reduced and fouling of the cellulose acetate membranes occurs because of the action of permeation drag.

Effect of Divalent Cations. The effect of Ca^{2+} ions on the permeate flux of both membranes is shown in Figure 8. Experiments were conducted at fixed particle concentration (30 mg/L) and background NaCl concentration (0.01 M). For both types of membranes, the presence of divalent calcium ions, at concentrations typical of natural and process waters, has no effect on the rate of fouling. The fouling of the composite membranes is much more significant than the fouling of the cellulose acetate membrane, mostly due to the higher initial permeation rate through the composite membranes. The fouling rate of the composite membranes is dominated by permeation drag, and double layer repulsion does not play a significant role. Unlike the composite

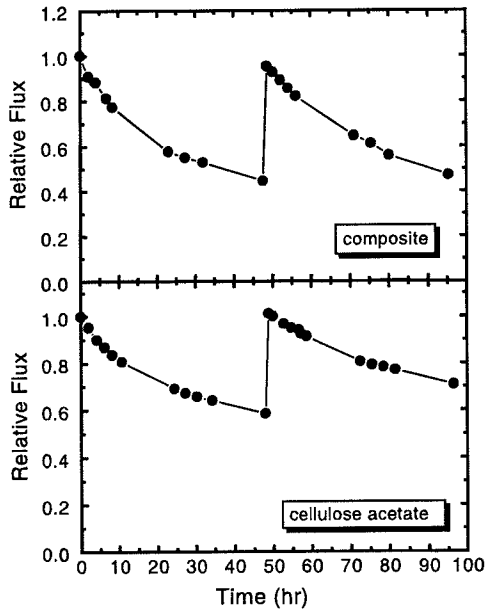

FIGURE 9. Relative flux as a function of time in reversibility experiments with composite and cellulose acetate RO membranes (see text for procedure). Experiments were conducted with 90 mg/L silica colloids and 0.1 M NaCl. Experiments with the composite membrane were carried out at pH 7.8 while those with the cellulose acetate membrane were carried out at pH 5.4–5.6. The initial fluxes for runs with the composite membranes were as follows: 8.04 × 10^{-6} m/s (before cleaning) and 7.65 × 10^{-6} m/s (after cleaning). The initial fluxes for runs with the cellulose acetate membranes were as follows: 5.95 × 10^{-6} m/s (before cleaning) and 6.02 × 10^{-6} m/s (after cleaning).

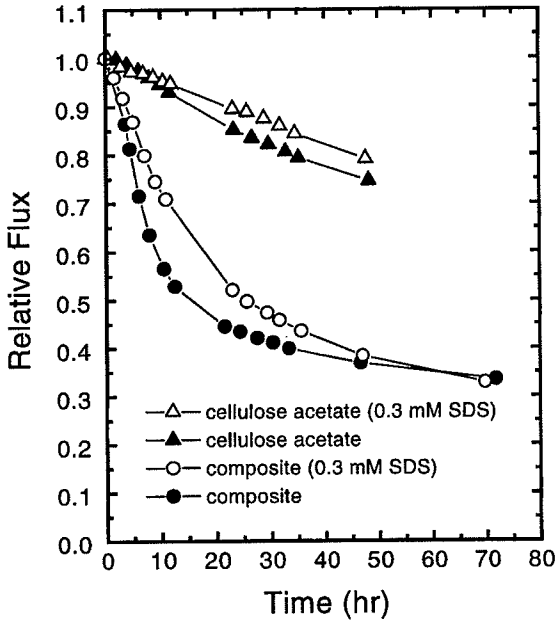

FIGURE 10. Relative permeate flux as a function of time for the composite and cellulose acetate RO membranes. Closed symbols are for fouling experiments with 0.01 M NaCl and open symbols are for fouling at 0.01 M NaCl plus 0.3 mM SDS. Silica colloid concentration was 90 mg/L. Experiments with the composite membrane were carried out at pH 7.8 while those with the cellulose acetate membrane were carried out at pH 5.4–5.6. The initial flux in all experiments was fixed at 1.1 × 10^{-5} m/s.

membranes, the permeation rate through the cellulose acetate membrane is lower and double layer repulsion hinders the deposition of silica colloids onto the membrane. While divalent cations may have a significant effect on the rate of particle deposition onto impermeable solid surfaces (*20*), their role in particle deposition onto membrane surfaces is less important because of the dominating effect of permeation drag. This unique coupling between physical (permeation drag) and chemical (double layer) interactions in particle deposition onto permeable membrane surfaces diminishes to some extent the importance of chemical interactions in colloidal fouling. It should be noted, however, that the observed results for the role of divalent cations in fouling cannot be generalized to other colloidal particles, since silica colloids are relatively stable (toward aggregation) even at the calcium ion concentrations used here (*12*).

Reversibility of Colloidal Fouling. In reversibility experiments, fouling tests similar to those described earlier were conducted for a period of 50 h. After 50 h of fouling, the operation of the RO unit was stopped for a short period of time during which the membranes were gently removed from the test cells and rinsed thoroughly by deionized water using a squeeze bottle. After rinsing the membranes and the cells, the membranes were placed back in the test cells and operation was resumed for an additional 50 h of fouling. The experiments were performed at high silica concentration (90 mg/L) and high ionic strength (0.1 M NaCl) at which fouling is significant.

Results of typical reversibility experiments with both membranes are shown in Figure 9. It is shown that, under the investigated chemical conditions, cleaning restores the permeate flux of the membranes. The results suggest that silica colloids do not bind irreversibly to the membrane surface, but rather deposit as a thick cake layer on the membrane surface. The thick fouling layer was clearly visible when the membranes were removed for rinsing. It was also seen that cleaning readily removed the colloid fouling layer from the membrane surface.

Comparison of Fouling Behavior of Composite and Cellulose Acetate RO Membranes. The fouling results presented so far clearly show that the cellulose acetate membranes have a lower fouling tendency than the thin-film composite membranes. Possible explanations for the differences in the fouling behavior may include lower permeate flux of the cellulose acetate membranes at the transmembrane pressures investigated, differences in the surface chemistry of the membranes, membrane surface charge heterogeneities, and differences in the surface roughness (morphology) of the membranes.

To eliminate the effect of permeation drag, the fouling behavior of the composite and cellulose acetate membranes was first compared at identical initial permeate fluxes. Furthermore, additional experiments were conducted in the presence of an anionic surfactant (sodium dodecyl sulfate, SDS) to mask differences in the surface chemistry of both membranes and to reduce inherent membrane surface charge heterogeneities. The colloidal fouling behavior of the membranes in the presence of 0.01 M NaCl (closed symbols) and 0.01 M NaCl plus 3 × 10^{-4} M SDS (open symbols) is presented in Figure 10.

The results shown in Figure 10 demonstrate that the fouling behavior of the composite and cellulose acetate membranes is considerably different. The flux through the cellulose acetate membrane decreases slowly throughout the entire fouling test whereas the flux through the composite membrane drops sharply during the first 12 h and later declines more gradually. Furthermore, the overall permeate flux reduction due to fouling is much greater with the composite membrane than the cellulose acetate membrane. Obviously, permeation drag can be ruled out as a cause for the different fouling behavior of the membranes since the initial permeate flux was identical (1.1 × 10^{-5} m/s) in the fouling experiments with both membranes. Hence, other explanations for the increased fouling rate of the composite membrane should be sought.

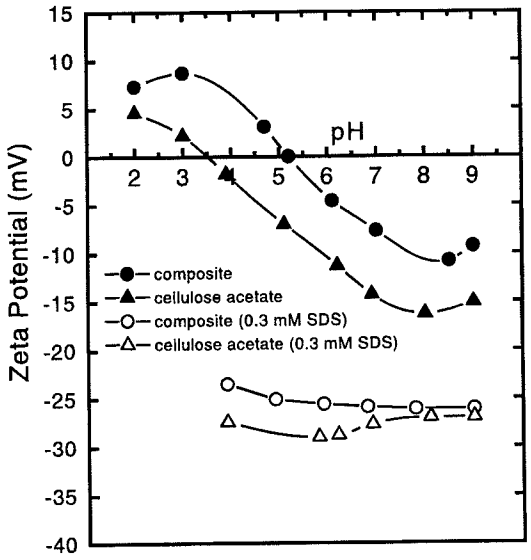

FIGURE 11. Zeta potential of the composite and cellulose acetate RO membranes as a function of solution pH. Closed symbols represent experiments with 0.01 M NaCl and open symbols represent experiments with 0.01 M NaCl plus 0.3 mM SDS.

Another possible cause for the different fouling behavior of the two types of membranes is surface chemical heterogeneity. Inherent local variations in the chemical nature of the polymer at the membrane surface can produce nonuniform distribution of surface charge and local variations in the hydrophobicity of the membranes. Theoretical analyses show that surface chemical heterogeneities can have a profound effect on the deposition rate of colloids onto stationary surfaces (*14, 21*).

Surface chemical heterogeneities of negatively charged surfaces can be masked by the addition of an anionic surfactant (*22, 23*). Adsorption of anionic surfactant molecules onto chemically heterogeneous surfaces results in a more uniform distribution of surface charge (*22*). The zeta potential results in Figure 11 indeed show that, in the presence of SDS, the membranes become much more negative and the difference between the zeta potential of the two membranes (as a result of differences between their surface chemistry) is eliminated. The striking effect of the anionic surfactant on the zeta potential of the membranes is attributed to adsorption of negatively charged surfactant molecules to the membrane surface (*22*). Surfactant molecules readily adsorb to the membrane surface and their negatively charged functional groups (sulfate in our case) dominate the membrane surface charge. However, the fouling results in the presence of SDS shown in Figure 10 reveal that the marked difference between the fouling behavior of the cellulose acetate and composite membranes still remains. There is a small decrease in the rate of fouling in the presence of surfactant due to increased electrostatic repulsion between colloids and between colloids and the membrane surface, but fouling is still significant.

It is evident that the only major remaining factor to explain the difference between the fouling behavior of the membranes is the marked difference in their surface morphology as shown earlier in Figure 2. Surface roughness of the type shown by the AFM images of the composite membranes produces tangential forces which can immobilize colloidal particles on the membrane surface (*24*). Furthermore, when a colloidal particle is in close vicinity of a rough membrane surface, the interaction can no longer be described by a single value of interaction energy; rather, a distribution of interaction energies should be considered (*14, 25*). These effects of surface roughness result in enhanced deposition of colloids onto the membrane surface (compared to the ideal case of a smooth membrane) and, hence, more severe fouling. A detailed discussion on the role of surface roughness in colloidal fouling of composite polyamide membranes is given elsewhere (*18, 26*).

Implications. The results reported in this paper demonstrate that permeation drag, which is determined by the membrane permeate flux, plays a paramount role in controlling the rate of colloid deposition onto membrane surfaces and subsequently the extent of membrane fouling. While conventional approaches favor operation of membrane systems at high permeate fluxes to obtain higher rates of product water, it may be more beneficial to operate RO systems processing source waters with high fouling potential at lower permeation rates to reduce membrane fouling. For a given source water, a threshold permeate flux below which colloidal fouling is significantly reduced may be found. This threshold flux will depend mostly on the chemical characteristics of the source water. Another important finding in this study is the role of surface roughness in membrane fouling. Membrane manufacturers should strive to synthesize polymeric membranes with smooth surfaces to further reduce membrane fouling. Lastly, because of the inherent permeation drag, fouling is inevitable for source waters with significant levels of colloids. Hence, research should focus on means to effectively clean fouled RO membranes or to optimize pretreatment of source waters.

Acknowledgments

We acknowledge the support of the State of California Department of Water Resources (Project B-58385), the National Water Research Institute (Project D-92-01), and the University of California Water Resources Center (Project P-92-9). Findings reported in this paper do not necessarily reflect the views of these agencies and no official endorsement should be inferred. We are also grateful to Nathan Lewis and Guruswany Kumaraswamy of the California Institute of Technology (Beckman Institute, Material Science Center) for allowing us to use their AFM.

Literature Cited

(1) AWWA Membrane Technology Research Committee. *J. Am. Water Works Assoc.* **1992**, *84*(*1*), 59–67.
(2) Potts, D. E.; Ahlert, R. C.; Wang, S. S. *Desalination* **1981**, *36*(3), 235–264.
(3) Stumm, W. *Chemistry of the Solid-Water Interface*; Wiley Interscience: New York, 1992.
(4) Zhu, X.; Elimelech, M. *J. Environ. Eng. ASCE* **1995**, *121*, 884–893.
(5) Belfort, G.; Davis, R. H.; Zydney, A. L. *J. Membr. Sci.* **1995**, *96*, 1–58.
(6) Winfield, B. A. *Water Res.* **1979**, *13*, 561–564.
(7) Winfield, B. A. *Water. Res.* **1979**, *13*, 565–569.
(8) Cohen, R. D.; Probstein, R. F. *J. Colloid Interface Sci.* **1986**, *114*, 194–207.
(9) Degussa Technical Bulletin No. 56. *Highly Dispersed Metallic Oxides Produced by the Aerosil Process.* Degussa Corp.: Akron, OH, 1990.
(10) Elimelech, M.; Chen, W. H.; Waypa, J. J. *Desalination* **1994**, *95*(3), 269–286.
(11) Childress, A. E.; Elimelech, M. *J. Membr. Sci.* **1996**, *119*, 253–268.
(12) Zhu, X. Ph.D. Dissertation, University of California, Los Angeles, 1996.
(13) Hunter, R. J. *Zeta potential in colloid science*; Academic Press: New York, 1981.
(14) Elimelech, M.; Gregory, J.; Jia, X; Williams, R. A. *Particle Deposition and Aggregation: Measurement, Modeling, and Simulation*; Butterworth-Heinemann: Oxford, 1995.
(15) Israelachvili, J. N. *Intermolecular and Surface Forces*, 2nd ed.; Academic Press: London, 1992.
(16) Vigil, G.; Xu, Z. H.; Steinberg, S.; Israelachvili, J. N. Interactions of Silica Surfaces. *J. Colloid Interface Sci.* **1994**, *166*, 367–385.
(17) Petersen, J. *J. Membr. Sci.* **1993**, *83*, 81–150.
(18) Elimelech, M.; Zhu, X.; Childress, A. E.; Hong, S. *J. Membr. Sci.* **1997**, *127*, 101–109.
(19) Song, L.; Elimelech, M. *J. Colloid Interface Sci.* **1995**, *173*, 165–180.

(20) O'Melia, C. R. *Colloids Surf.* **1989**, *39*, 255–271.
(21) Song, L.; Johnson, P. R.; Elimelech, M. *Environ. Sci. Technol.* **1994**, *28*, 1164–1171.
(22) Litton, G. M.; Olson, T. M. *J. Colloid Interface Sci.* **1994**, *165*, 522–526.
(23) Hull, M.; Kitchener, J. A. *Trans. Faraday Soc.* **1969**, *65*, 3093–3104.
(24) Adamczyk, Z.; Czarnecki, J.; Dabros, T.; van de Ven, T. G. M. *Adv. Colloid Interface Sci.* **1983**, *19*, 183–252.
(25) Bowen, B. D.; Epstein, N. *J. Colloid Interface Sci.* **1979**, *72*, 81–97.
(26) Childress, A. E. Ph.D. Dissertation, University of California, Los Angeles, 1997.

Received for review May 7, 1997. Revised manuscript received August 27, 1997. Accepted August 29, 1997.[⊗]

ES970400V

[⊗] Abstract published in *Advance ACS Abstracts,* October 15, 1997.